Directional bilateral asymmetry in otolith morphology may affect fish stock discrimination based on otolith shape analysis

Kélig Mahé[1,*], Djamila Ider[2], Andrea Massaro[3], Oussama Hamed[4], Alba Jurado-Ruzafa[5], Patrícia Gonçalves[6], Aikaterini Anastasopoulou[7], Angelique Jadaud[8], Chryssi Mytilineou[7], Romain Elleboode[1], Zohir Ramdane[2], Mahmoud Bacha[9], Rachid Amara[9], Hélène de Pontual[10], and Bruno Ernande[1]

[1]Fisheries Laboratory, IFREMER, 150 Quai Gambetta, BP 699, 62 321 Boulogne-sur-Mer, France
[2]Laboratoire de Zoologie Appliquée et d'Ecophysiologie Animale, Université Abderrahmane Mira, Béjaïa, Algérie
[3]APLYSIA – Via Menichetti 35, 27121 Livorno, Italy
[4]Université de Tunis El Manar, Campus Universitaire, 2092 El Manar II, Tunisie
[5]Instituto Español de Oceanografía, Centro Oceanográfico de Canarias, 38180 Santa Cruz de Tenerife, Spain
[6]Departamento do Mar e Recursos Marinhos, Intituto Português do Mar e da Atmosfera (IPMA), Lisboa, Portugal
[7]Hellenic Centre for Marine Research, PO Box 712, P.C. 19013, Anavyssos Attiki, Athens, Greece
[8]Fisheries Laboratory, IFREMER-UMR MARBEC, Avenue Jean Monnet, CS 30171, 34203 Sète Cedex, France
[9]Laboratoire d'Océanologie et de Géosciences, Université Littoral Côte d'Opale, Univ. Lille, CNRS, UMR 8187, LOG, F 62930 Wimereux, France
[10]IFREMER, Sciences et Technologies Halieutiques, CS 10070, 29280 Plouzané, France

*Corresponding author: tel: +0033 321995602; e-mail: kelig.mahe@ifremer.fr.

Otolith shape analysis is an efficient fish stock identification tool. However, most applications used left and right otoliths or only one of them arbitrarily chosen without testing for biases resulting from potential directional bilateral asymmetry (DA) in otolith shape, i.e. a unimodal population-level deviation form bilateral symmetry between right and left otolith shapes. In this study, 560 bogues (Boops boops) were sampled from 11 geographical locations from the Canary Islands to the Aegean Sea and elliptical Fourier descriptors were used to describe their otoliths' shape. First, a significant otolith DA was observed at the global scale with an average amplitude of 2.77%. However, at the scale of sampling locations, DA was not always significant and varied in amplitude and direction. Second, population structure was investigated using the shape of either right otoliths or left otoliths or both together. Analyses based on right otoliths or both otoliths together, suggested three stock units: a North-Western Mediterranean Sea stock, an Eastern Mediterranean Sea stock, and a Central-Eastern Atlantic Ocean and South-Western Mediterranean Sea stock. In contrast, no coherent geographical pattern was found based on left otoliths. Our results highlight the importance of accounting for potential otolith DA in otolith shape-based stock identification.

Keywords: Boops boops, elliptical Fourier analysis, Mediterranean Sea, side effect, stock identification.

Introduction

Stock identification and the knowledge of population spatial structure provide a basis for understanding fish population dynamics and achieving reliable assessments for fishery management (Reiss et al., 2009). Some studies suggested that a lack of knowledge of population spatial structure in fisheries management might be responsible for fishery collapses [e.g. Atlantic cod (Gadus morhua) in the Western Atlantic, Hutchings,

2005; the crustacean fisheries of Alaska, Wooster, 1992; North-Western Atlantic herring, Stephenson et al., 1999]. Therefore, a wide number of techniques was developed and applied to identify and discriminate stock units, such as tagging experiments or analyses of spatial variation in arrange of markers including genetic markers, morphological traits, life-history traits at various life-stages, parasite load or infracommunity structure, or contaminant concentration (Pawson and Jennings, 1996; Garcia et al., 2011; Cadrin et al., 2014; ICES, 2016, Pita et al., 2016). Otoliths are calcified structures overlying the sensory epithelia in the inner ears. The left and right inner ear contain three pairs of otoliths each. They grow throughout the life of the fish and, unlike scales and bones, are metabolically inert (i.e. once deposited, otolith material is unlikely to be resorbed or altered, Casselman, 1987). Consequently, otolith shape remains unaffected by short-term changes in fish condition (Campana and Casselman, 1993) or environmental variations (Campana, 1999). Shape analysis was first used to discriminate fish stocks by using either scales of Atlantic salmon (Salmo salar) (de Pontual and Prouzet, 1987, 1988) or otolith of Atlantic cod (Campana and Casselman, 1993). Since then, many studies have focused on otolith-shape analysis to discriminate between stock units, reaching an updated total of 91 papers published from 1993 to 2017 exclusively on this topic.

The shape of a fish's otolith depends on its genotype, its developmental stage (potentially described by a series of individual-state variables such as body size, age, sex, and sexual maturity status) and both the biotic and abiotic environments encountered during its lifetime (Castonguay et al., 1991; Lombarte and Lleonart, 1993; Cadrin and Friedland, 1999; Begg and Brown, 2000; Cardinale et al., 2004; Gagliano and McCormick, 2004; Monteiro et al., 2005; Swan et al., 2006; Mérigot et al., 2007; Hüssy, 2008; Vignon and Morat, 2010; Capoccioni et al., 2011; Mille et al., 2016). Besides inter-individual variation, otolith shape is also known to vary potentially intra-individually as left otolith shape may not be perfectly symmetrical to right otolith shape one and vice versa (Díaz-Gil et al., 2015). Such deviation or bilateral asymmetry can be of three different types corresponding to three different distributions of its individual values within a population (Palmer and Strobeck, 1986, 1992). Fluctuating asymmetry (FA) corresponds to random individual deviations from perfect bilateral symmetry resulting in a normal distribution with mean 0. FA in otolith shape has been reported for some species of both roundfish and flatfish (Lemberget and McCormick, 2009; Lychakov, 2013; Díaz-Gil et al., 2015). Directional asymmetry (DA) relates to a systematic deviation from bilateral symmetry towards one side (e.g. the otolith asymmetry in flatfish, Mille et al., 2015) and is thus characterized by a normal distribution with a mean different from 0 whose sign depends on the side of the deviation. Antisymmetry (A) occurs when there is a systematic but alternating deviation towards one side or the other in the population, thus generating a bimodal distribution with mean 0 in its extreme form (e.g. of the claws of fiddler crabs Palmer and Strobeck, 1986; or lobsters Govind and Pearce, 1986). If DA or A occurs, it may affect the results of otolith shape-based stock discrimination, depending on which otolith is used. Among the 91 published studies on marine fish stock identification based on otolith shape analysis, only 20 of them took into account otolith shape asymmetry (A) and only three based their analyses on the two otoliths together. Most studies arbitrarily used otoliths from only one side. In this context, the first objective of this study was

to explore the effect of DA in otolith morphology on stock identification based on otolith shape analysis.

To describe the external contour or shape of otoliths, several techniques have been developed: univariate descriptors such as shape factors that include roundness or circularity (Tuset et al., 2003), geometric morphometrics (Ponton, 2006; Ramirez-Perez et al., 2010; Vergara-Solana et al., 2013), wavelet functions (Parisi-Baradad et al., 2005; Sadighzadeh et al., 2014), growth markers (Benzinou et al., 2013), curvature scale space (Mapp et al., 2013), and geodesic methods (Benzinou et al., 2013). However, the elliptical Fourier analysis (EFA) remains the most widely used method to describe otolith shape. In recent years, the number of studies using EFA has increased substantially and allowed the analysis of population structure of as diverse species as highly migratory oceanic swordfish (Xiphias gladius; Mahé et al., 2016) and sedentary big-scale sand smelt (Atherina boyeri; Boudinar et al., 2015).

In this paper, we used the bogue (Boops boops; Linnaeus, 1758), a species within the Sparidae family, as a case study for assessing the effect of DA and/or A on stock identification based on otolith shape analysis using EFA. This species has a wide geographical distribution from the Norwegian to Angolan coasts along the northeastern Atlantic, as well as in the Mediterranean and Black Seas (Whitehead et al., 1984). Bogue is both demersal and semi-pelagic and inhabits all types of seabed (sand, mud, rock, and seagrass beds) down to 350 m depth, but is most abundant in the upper 100 m. It is an important species for Mediterranean fisheries with an average landing of 27 000 tons from 2010 to 2013 (ranked 7th and accounting for 1.8% of total catches in the Mediterranean Sea, FAO, 2016). This species is currently fully exploited by several commercial fisheries, as either a target species or bycatch, mainly from pelagic trawlers (FAO, 2016; Dimarchopoulou et al., 2017). Moreover, although bogue is one of the seven most studied species in the Mediterranean Sea (Dimarchopoulou et al., 2017), no information is available on its general stock structure. Hence, the second objective of this study was to investigate the stock structure of the bogue in the Mediterranean Sea and the adjacent area of the Atlantic Ocean.

To reach the two objectives of this study, i.e. (i) to explore the impact of otolith DA on otolith shape-based stock identification and (ii) to investigate bogue stock structure in the Mediterranean Sea, we extract left and right otolith shape using elliptical Fourier descriptors and use them to, first, test for otolith DA and investigate how its varies across sampling locations and, second, investigate stock structure through a combination of linear discriminant analysis (LDA) and clustering using sequentially the shape of left otoliths only, rights otoliths only and both together.

Material and methods
Sample collection
Sagittal otoliths (left and right) were extracted from a total of 560 individuals ranging from 13 to 26 cm total length (mean ± s.e.: 18.38 ± 2.63 cm), collected from 11 locations from the Canary Islands to the Aegean Sea (Figure 1 and Table 1). Samples were collected between 2013 and 2016 by six Institutes (Institut Français de Recherche pour l'Exploitation de la Mer—IFREMER, France; University Abderrahmane Mira, Algeria; APLYSIA institute, Italy; University of Tunis, Tunisia; Instituto Español de Oceanografía—IEO, Spain; Hellenic Centre for Marine Research-HCMR, Greece) during the international bottom trawl survey in the Mediterranean

Figure 1. Map of sampling locations of bogues (1: Tenerife Island, 2: Gulf of Oran, 3: Gulf of Bejaia, 4: Gulf of Annaba, 5: Gulf of Tunis, 6: Gulf of Lions, 7: Corsica Island, 8: Ligurian Sea, 9: Tyrrhenian Sea, 10: Ionian Sea, 11: Aegean Sea).

Sea (MEDITS surveys), on board fishing vessels and from fish markets. The sex of the sampled individuals was determined by macroscopic examination of their gonads and only mature fish were included in this study to minimize the effect of sexual maturity, which may affect otolith shape (Cardinale *et al.*, 2004). Moreover, to limit the effect of age on the otolith shape, the age range of fish sampled was limited from 2 to 4 years. To estimate the age of each individual, whole sagittal otoliths were examined, after cleaning, by two expert age readers to limit interpretation errors. To increase the visibility of the growth marks, otoliths were covered with clove essential oil and observed with a stereomicroscope under reflected light on a dark background.

Otolith shape analysis

A calibrated high-resolution image (3.200 dpi) of the proximal face of the whole left and right sagittal otolith was obtained using a scanner with reflected light (Epson V750). During this process, a fixed single magnification was used to ensure as high a resolution as possible. Image processing was performed using the image analysis system TNPC (Digital processing for calcified structures, version 7) with the *sulcus acusticus* facing up. To compare left and right otolith shapes, mirror images of left otoliths were used. The length and width of otoliths were automatically extracted as the largest distance along the antero-posterior axis and the ventro-dorsal axis, respectively.

To describe otolith contours, elliptic Fourier analysis (Lestrel, 2008) was carried out on each otolith contour delineated and extracted after image binarization. All elliptic Fourier descriptors (EFDs) were obtained by using TNPC 7 software. For each otolith, the first 99 elliptical Fourier harmonics (H) were extracted and normalized with respect to the first harmonic and were thus invariant to otolith size, rotation, and starting point of contour description (Kuhl and Giardina, 1982). To determine the number of harmonics required to reconstruct the otolith outline, the cumulated Fourier Power (F) was calculated for each individual otolith as a measure of the precision of contour reconstruction obtained with n_k harmonics (i.e. the proportion of variance in contour coordinates accounted for by the n_k harmonics):

Table 1. Sampling scheme.

Geographical area	Number	Total length (cm) mean ± s.e.	Year sampling
Canary Islands	*67*	*19.00 ± 0.93*	*2016*
1: Tenerife Island	67	19.00 ± 0.93	2016
Algeria	*179*	*16.25 ± 3.25*	*2013/2014/ 2015/2016*
2: Gulf of Oran	47	15.50 ± 0.71	2015
3: Gulf of Bejaia	92	15.06 ± 1.70	2013/2014
4: Gulf of Annaba	40	19.12 ± 4.52	2016
Tunisia	*48*	*18.50 ± 1.02*	*2016*
5: Gulf of Tunis	48	18.50 ± 1.02	2016
France	*95*	*19.89 ± 3.75*	*2016*
6: Corsica Island	41	18.50 ± 1.91	2016
7: Gulf of Lions	54	21.00 ± 4.69	2016
Italy	*109*	*18.91 ± 1.91*	*2015*
8: Ligurian Sea	50	19.00 ± 1.74	2015
9: Tyrrhenian Sea	59	18.82 ± 2.07	2015
Greece	*62*	*19.23 ± 2.65*	*2014*
10: Ionian Sea	35	16.80 ± 2.86	2014
11: Aegean Sea	27	20.75 ± 0.71	2014

The number of sampled individuals (Number), their total length (mean and standard deviation), and the sampling years are given by geographical area and year.

$$F_{(n_k)} = \sum_{i=1}^{n_k} \frac{A_i^2 + B_i^2 + C_i^2 + D_i^2}{2},$$

where A_i, B_i, C_i, and D_i are the coefficients of the H_i harmonic. $F(n_k)$F and n_k were calculated for each individual otolith k to ensure that each individual otolith in the sample was reconstructed with a precision of 99.99% (Lestrel, 2008). The maximum number of harmonics $n = \max(n_k)$ across all otoliths was then used to reconstruct each individual otolith.

Statistical analyses

DA in otolith shape was analysed as the effect of otolith's location side, i.e. left vs. right inner ear (side *SI*, thereafter) on otolith shape. First, principal components analysis (PCA) was applied to the selected elliptical Fourier descriptors (EFDs) matrix (*EFDs* as columns and individual otolith as lines) of otolith contours (Rohlf and Archie, 1984) and a subset of the resulting principal components (PCs) was selected as otolith shape descriptor according to the broken stick model (Legendre and Legendre, 1998). The matrix of selected PCs, with PCs as columns and otoliths as lines, is referred to as the shape matrix *S* hereafter. This procedure allowed us to decrease the number of variables used to describe otolith shape variability while ensuring that the main sources of shape variation were accounted for, as well as to avoid co-linearity between shape descriptors (Rohlf and Archie, 1984).

The shape matrix (*S*) was analysed using the following multivariate mixed-effects model:

$$S \sim L + SI + LO + SI : LO + i,$$

where otolith shape variations due to side (*SI*), sampling location (*LO*), and their interaction (*SI* : *LO*) are represented by fixed effects. More precisely, *SI* measures DA at the global scale,

LO assesses shape variation across sampling locations affecting both otoliths, and SI : LO represents variation in DA across sampling locations. Individuals' total length L was also included as a covariate to remove some potentially confounding ontogenetic effect on otolith shape. Finally, a random intercept (i) was used to account for variability due to individuals (or some of their characteristics, such as total length for instance) and autocorrelation between left and right otolith shapes within individuals. The model was fitted with a different variance for each PC of the shape matrix S. Normality of the residuals and the random effects as well as homoscedasticity of the residuals were assessed by visual inspection of diagnostic plots. The significance of explanatory variables at 5% was tested by likelihood ratio tests between nested models while respecting marginality of the effects (type 2 tests; Fox and Weisberg, 2011) that are supposed to follow a χ^2 distribution under the null hypothesis. To visualize differences in otolith shape between right and left sides, an average otolith shape was rebuilt for each side based on EFDs. Moreover, the direction and amplitude of DA at the global scale and at each sampling location was extracted from the multivariate mixed-effects model as the estimators of the side effect SI and of the interaction between head side and sampling location SI : LO, respectively. To ease interpretation, it was also evaluated as the average percentage of non-overlapping surface between the right and left otoliths' shapes reconstructed on the basis of the EFDs at the individual level. The percentage was computed relative to the total area.

To discriminate fish from the 11 sampled locations based on otolith shape, a LDA with jacknifed prediction was applied to the residuals R_S of a redundancy analysis (RDA) $S \sim L$ of the shape matrix S explained by individuals' total length L. The use of the residual matrix R_S instead of the shape matrix S was meant to avoid potential confounding effects due to otolith shape variation across sampling locations related to variations in individuals' size originating from different size-selectivity of the capture procedure/gear at different sampling sites (Rencher and Christensen, 2012). To evaluate the resulting discriminant functions, the percentage of correct classification of individuals into sampling areas was calculated using jacknife cross-validation (Klecka, 1980) and compared to those obtained from random distribution. Moreover, the performance of the discriminant analyses was assessed using the Wilks' λ. This value is the ratio between the intra-group variance and the total variance, and provides an objective way of calculating the percentage of agreement between real and predicted groups' membership. Wilks' λ values range from 0 to 1 and the closer to 0, the better the discriminating power of the RDA. To complete the stock identification procedure, a cluster analysis according to Ward's hierarchical agglomerative algorithm based on squared Euclidean distances was performed on the residual shape matrix R_S to group individuals with similar otolith shapes. These analyses were carried out three times: on left otoliths only, on right otoliths only, and on both.

Statistical analyses were performed using the following packages in the statistical environment R (R Development Core Team, 2016): "nlme" (Pinheiro et al., 2016), "Effects" (Fox, 2003), "Vegan" (Oksanen et al., 2013), "SP" (Bivand et al., 2013), "ggplot2" (Wickham, 2016), "RGEOS" (Bivand et al., 2013), "MASS" (Venables and Ripley, 2002), and "RRCOV" (Todorov and Filzmoser, 2009).

Table 2. Results of the multivariate mixed-effects model on the shape matrix S.

Variable	χ^2	df	p
TL	422.599	7	<0.001
SI	34.580	7	<0.001
LO	96.822	7	<0.001
SI:LO	121.923	7	<0.001

For each explanatory variable, the χ^2 statistic, the associated degrees of freedom (df) and the resulting p-value (p) for a type II test are given. *<0.05; **<0.01, ***<0.001.

Results

Directional asymmetry in otolith shape

Among the 99 Fourier harmonics extracted to describe individual otolith contours, the first 26 harmonics explained at least 99.99% of the variation in otolith contour of each individual and were thus used for further analysis. After PCA on the EFDs, only the first six PCs were kept for the shape matrix S according to the broken-stick model (which, in this case, corresponded to a threshold of 2.4% of the total variance explained; Borcard et al., 2011). These six PCs explained 78% of the total variance in the EFDs.

The multivariate mixed-effects model on the shape matrix S showed that there was a significant DA between left and right otolith shapes at the global scale (Table 2, SI effect) with a consistent bias towards the right side (Supplementary Figure S1). The amplitude of DA, measured as the percentage of the non-overlapping surface between the right and left otolith shapes, was on average equal to 2.77% among all sampling sites. However, there was also a significant effect of the interaction between side and sampling location on otolith shape (Table 2; SI : LO effect) indicating that the amplitude and/or the direction of DA varied across sampling locations. More precisely, the amplitude of DA varied between 1.25 and 4.66% depending on the sampling site (Figure 2) and was significant in only 5 of them, located along the Algerian and Italian coasts. The main shape difference between left and right otoliths was located between the rostrum and the antirostrum has shown by average left and right otoliths shape reconstruction at each sampling location (Figure 2). In addition to its amplitude, the direction of DA also varied according to the considered location (Figure 2). Among the sampling locations with a significant DA, the right otolith presented a width/length ratio larger than the left one in the Ligurian and Tyrrhenian Seas whereas it was the reverse in the Gulfs of Oran, Bejaia, and Annaba (Figure 2; Supplementary Table S1).

Fine-grained geographical structuring of otolith shape

The effect of sampling location on otolith shape was significant in the multivariate mixed effects model (Table 2, LO effect) suggesting geographical variation in otolith shape that could used to discriminate individuals from different geographical origins Sampling location was therefore used as an explanatory variable in the subsequent otolith shape-based LDA. In contrast with the previous analyses, the procedure to produce the otolith shape matrix S was performed separately for left and right otoliths. The first six PCs after PCA on the first 26 harmonics EFDs were selected for the corresponding left and right shape matrices S_L and
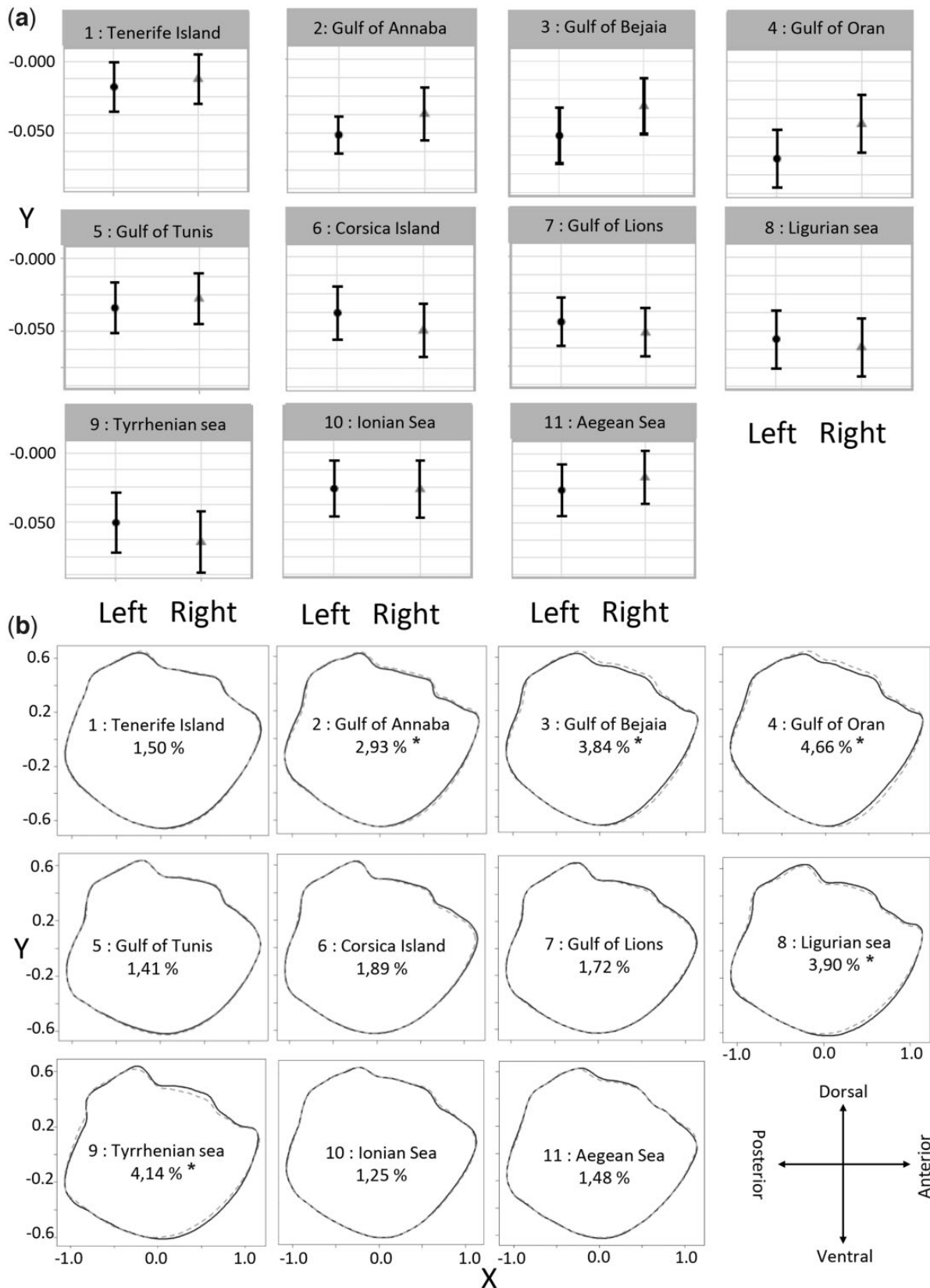
Figure 2. (a) Directional asymmetry between left and right otolith shapes at each sampling location as estimated by the interaction between side and sampling location in the multivariate mixed-effects model. Black dots and grey triangles represent the estimator for the left and right otoliths, respectively, and vertical bars are there 95% confidence intervals. Percentage given in each panel is the average percentage of non-overlapping surface between the two reconstructed otolith shapes at the individual level. (b) Difference between right (black line) and left (grey dotted line) otolith shapes for each geographical location as shown by average shape reconstruction for each sampling location based on EFDs. Percentages are the average percentages of non-overlapping surface between the two reconstructed otolith shapes at the individual level (*<0.05).

Table 3. Jackknifed correct classification matrix of the linear discriminant analysis for left otoliths ($n = 560$) between the 11 sampling areas based on the residual shape matrix R_{S_L}.

| | | Predicted area | | | | | | | | | | | |
		1: Tenerife	2: Oran	3: Bejaia	4: Annaba	5: Tunis	6: Lions	7: Corsica	8: Ligurian	9: Tyrrhenian	10: Ionian	11: Aegean	% correct
Actual area	1: Tenerife	18	4	24	4	8	3	0	1	0	0	5	27%
	2: Oran	0	16	29	1	0	0	0	1	0	0	0	34%
	3: Bejaia	10	8	61	1	2	5	0	4	0	0	1	66%
	4: Annaba	0	5	10	12	3	2	0	8	0	0	0	30%
	5: Tunis	9	0	8	2	22	4	1	1	0	0	1	46%
	6: Lions	3	2	10	2	6	17	4	10	0	0	0	31%
	7: Corsica	1	0	4	3	3	9	12	8	1	0	0	29%
	8: Ligurian	0	0	12	3	3	4	2	22	4	0	0	44%
	9: Tyrrhenian	6	0	12	11	1	5	2	10	12	0	0	20%
	10: Ionian	3	4	4	0	2	1	1	1	0	6	13	17%
	11: Aegean	3	1	3	1	3	0	0	4	0	5	7	26%
	Total	53	40	177	40	53	50	22	70	17	11	27	37%

The number in each cell represents the number of individuals of the area of origin corresponding to the cell row classified into the predicted area corresponding to the cell column.

Table 4. Jackknifed correct classification matrix of the linear discriminant analysis for right otoliths ($n = 560$) between the 11 sampling areas based on the residual shape matrix R_{S_R}.

| | | Predicted area | | | | | | | | | | | |
		1: Tenerife	2: Oran	3: Bejaia	4: Annaba	5: Tunis	6: Lions	7: Corsica	8: Ligurian	9: Tyrrhenian	10: Ionian	11: Aegean	% correct
Actual area	1: Tenerife	31	3	12	2	8	2	6	1	0	1	1	46%
	2: Oran	4	22	20	1	0	0	0	0	0	0	0	47%
	3: Bejaia	7	9	65	1	0	5	1	1	1	2	0	71%
	4: Annaba	2	1	21	6	0	8	0	2	0	0	0	15%
	5: Tunis	6	0	1	1	27	4	3	1	3	0	2	56%
	6: Lions	7	1	2	0	5	25	8	3	2	0	1	46%
	7: Corsica	8	0	1	1	2	12	4	9	3	0	1	10%
	8: Ligurian	1	1	5	1	5	10	8	8	9	1	1	16%
	9: Tyrrhenian	0	0	1	0	2	17	14	11	13	1	0	22%
	10: Ionian	2	1	2	0	3	0	1	2	1	12	11	34%
	11: Aegean	2	0	3	1	4	0	3	3	0	7	4	15%
	Total	70	38	133	14	56	83	48	41	32	24	21	39%

The number in each cell represents the number of individuals of the area of origin corresponding to the cell row classified into the predicted area corresponding to the cell column.

S_R. After removal of the effect of individuals' total length L by a RDA on S_L and S_R to obtain residual shape matrices R_{S_L} and R_{S_R}, the overall jacknifed classification success of the LDA was 37% for the left otoliths and 39% for the right ones (Tables 3 and 4). The analysis confirmed significant differences between sampling sites for otoliths of both sides (left otoliths: Wilks' $\lambda = 0.426$; $F_{2\ 860}^{60} = 10.13$; $p < 0.001$; right otoliths: Wilks' $\lambda = 0.351$; $F_{2\ 860}^{60} = 12.97$; $p < 0.001$). For left otoliths, the misclassified individuals were distributed across all locations (Table 3) whereas, for right otoliths, they were segregated between two main groups: North-Western Mediterranean Sea vs. other locations (Table 4).

Clustering on otolith shape

The hierarchical clustering analysis identified three clusters for left and right otoliths (Table 5). No geographical coherence was identified for the three clusters of the left otoliths (Table 5). However, for right otoliths, the predicted areas coincided with (i) the north-western part of the Mediterranean Sea (Gulf of Lions, Corsica, Northern Ligurian Sea, and Southern Ligurian Sea), (ii) a large continuum composed of the central-eastern Atlantic Ocean (Tenerife Island) and the South-Wwestern part of Mediterranean Sea (Gulfs of Oran, Bejaia, Annaba, and Tunis), and (iii) the eastern part of the Mediterranean Sea (Ionian Sea and Aegean Sea) (Table 5). The same analyses as above were repeated but using the shape of otoliths of both sides at the same time. The results corroborated those obtained when using the right otoliths only. First, the overall jacknifed classification success was 39%, similar to the one obtained with the right otoliths (Supplementary Table S2; Table 4). Second, the hierarchical clustering analysis identified the same three geographically coherent clusters (Supplementary Table S2; Table 5).

Stock structure inferred from otolith shape

The stock structure was investigated using right and left otoliths together. Combining the geographical areas into two stocks, the North-Western Mediterranean Sea and the rest consisting of the

Table 5. Classification matrix resulting from hierarchical clustering on the residual shape matrix for left otoliths R_{S_L} and right otoliths R_{S_R} ($n = 560$) between the 11 sampling areas.

Area	Left otolith			Right otolith			Total
	Cluster 1	Cluster 2	Cluster 3	Cluster 1	Cluster 2	Cluster 3	
1: Tenerife Island	53	14		60	4	3	67
2: Gulf of Oran	36	11		38	1	8	47
3: Gulf of Bejaia	74	18		81	5	6	92
4: Gulf of Annaba	18	22		25	10	5	40
5: Gulf of Tunis	12	36		27	20	1	48
6: Gulf of Lions	26	26	2	25	27	2	54
7: Corsica Island	19	19	3	11	29	1	41
8: Ligurian Sea	35	23	2	28	29	3	60
9: Tyrrhenian Sea	15	32	2	20	28	1	49
10: Ionian Sea	29	6		32	3		35
11: Aegean Sea	17	10		18	9		27
Total	334	217	9	365	165	30	560

For each area, the cluster gathering the highest number of individuals is highlighted by a shaded cell.

Atlantic Ocean and the South-Western Mediterranean Sea, 72% of individuals were assigned correctly by the LDA. However, the overall classification success was the same when integrating the Central and Eastern Mediterranean Sea (Gulf of Tunis, Aegean, and Ionian Seas) in either of the two previous stocks. The best overall classification success (Wilks' $\lambda = 0.525$; $F^{12}_{1\ 106} = 40.13$; p-value < 0.001; Correct classification rate $= 86\%$) was obtained with three stocks units consisting in:
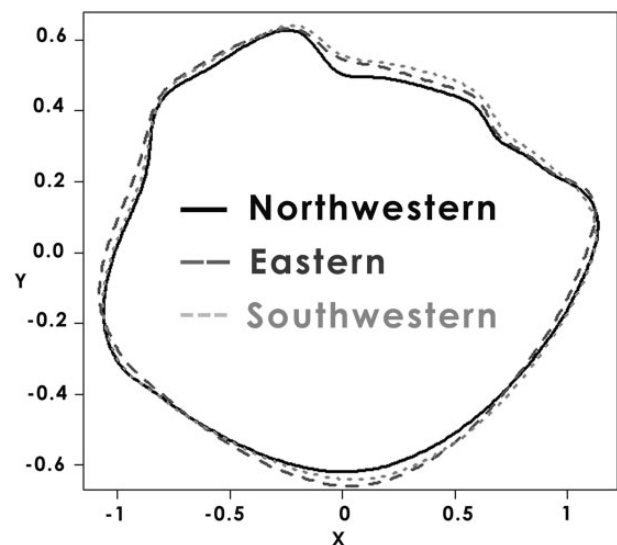
- the North-Western Mediterranean Sea (from the Gulf of Lions to the Tyrrhenian Sea),
- the Central-Eastern Atlantic Ocean and South-Western Mediterranean Sea (from the Canary Islands to Gulf of Tunis), and
- the Eastern Mediterranean Sea (from the Ionian Sea to Aegean Sea).

The otoliths from the North-Western Mediterranean Sea presented a lower width/length ratio than that of the otoliths from the southern part of the Mediterranean Sea and the Atlantic Ocean. The otoliths from the Eastern Mediterranean Sea were closer to those from the southern part of the Mediterranean Sea than to those from the North-Western Mediterranean Sea in terms of shape (Figure 3). This split into three stocks using both right and left otoliths dataset together was also coherent when using right otoliths' shape (Wilks' $\lambda = 0.627$; $F^{12}_{1\ 106} = 31.71$; p-value < 0.001; Correct classification rate $= 75\%$), whereas it was not when left otoliths' shape (Wilks' $\lambda = 0.741$; $F^{12}_{1\ 106} = 30.45$; p-value $= 0.081$, Correct classification rate $= 47\%$).

Discussion
Effect of confounding factors on the otolith shape
The otolith shape of fish from different geographical origins is affected by both abiotic environmental parameters (e.g. temperature, salinity) and biotic parameters such as prey availability, and is dependent on individual genotype (Campana and Casselman, 1993; Cadrin and Friedland, 1999; Torres *et al.*, 2000; Cardinale *et al.*, 2004; Gagliano and McCormick, 2004; Swan *et al.*, 2006; Vignon and Morat, 2010). Consequently, a combination of both environmental and genetic variation generates the morphological

Figure 3. Difference among average reconstructed otolith shapes between the three identified stock units: North-Western Mediterranean Sea (solid line; from the Gulf of Lions to the Tyrrhenian Sea), Eastern Mediterranean Sea (dashed line; from the Ionian Sea to the Aegean Sea), and Southwestern Mediterranean Sea and Atlantic Ocean (dotted line; from the Canary Islands to the Gulf of Tunis).

differences in otolith shape that may allow the discrimination of stock units. However, the factors that influence the shape are not fully understood and have not been investigated deeply yet (Burke *et al.*, 2008). A recent study showed that the ontogenetic trajectory of otolith shape could be affected by the environmental disturbance during early life stage (Vignon, 2018). Other studies have attributed shape differences to fish length (Smith, 1992; Campana and Casselman, 1993; Mérigot *et al.*, 2007), age (Bird *et al.*, 1986), year-class (Castonguay *et al.*, 1991; Campana and Casselman, 1993; Bolles and Begg, 2000; Mapp *et al.*, 2017), sexual maturity (Campana and Casselman, 1993; Cardinale *et al.*, 2004), and sexual dimorphism (Campana and Casselman, 1993; Bolles and Begg, 2000). More specifically, otolith shape has been reported to be

related to fish growth and thus subsequently size (Campana and Casselman, 1993). Furthermore, ontogenic changes in otolith shape, also often measured as size-related variation, have been shown to arise from variability in growth rates depending on habitat quality and the developmental processes (Simoneau *et al.* 2000; Monteiro *et al.,* 2005). In addition, the formation of a secondary growth centre and/or the appearance of checks in response to stress conditions can modify the otolith shape and the level of crenulation during the early life stages (Campana and Neilson, 1985; Massou *et al.,* 2004; Hüssy, 2008; Vignon, 2018). Consequently, the complexity of the otolith outline increases with the ontogenetic stage of the fish. To limit this effect, sampling can be restricted to a specific life-stage and/or to a narrow length range. If these factors are not taken into account, results of otolith shape-based stock discrimination might be biased. This is the reason why all analyses in this study were carried out on adults of 2–4 years old within a limited size range. In addition, the effect of individuals' total length was systematically accounted for.

Directional bilateral asymmetry in otolith shape

Our results show that DA can be observed in otolith shape in roundfishes such as bogue. DA between right and left otolith shapes was previously described for other roundfish species such as *Liza ramada* (Rebaya *et al.,* 2017), *Diplodus annularis* (Trojette *et al.,* 2015), *Diplodus puntazzo* (Bostanci *et al.,* 2016), *Clupea harengus* (Bird *et al.,* 1986), and *Scomberomorus niphonius* (Zhang *et al.,* 2016). Conversely, symmetry between left and right otolith shapes was observed for other fish species: *Gadus morhua* (Cardinale *et al.,* 2004; Petursdottir *et al.,* 2006), *Synechogobius ommaturus* (Wang *et al.,* 2011), *Coryphaena hippurus* (Duarte-Neto *et al.,* 2008), *Xiphias gladius* (Mahé *et al.,* 2016), *Scomber scombrus* (Castonguay *et al.,* 1991), and *Lutjanus kasmira* (Vignon and Morat, 2010). Although these studies tested for DA in roundfishes (and sometimes detected), they never studied it in detail.

DA has also been reported for flatfish species, such as *Solea solea* (Mérigot *et al.,* 2007; Mille *et al.,* 2015), *Limanda limanda* and *Lepidorhombus whiffiagonis* (Mille *et al.,* 2015). Otolith DA is expected in flatfishes and could arise during their early life, particularly after the cranial deformation and the migration of one eye to the other side caused by cell proliferation in suborbital tissue during metamorphosis at the larval stage (Bao *et al.,* 2011). This lateralization process may induce the difference in otolith biomineralization (carbonate accretion rates) often observed between the two inner ears of flatfishes, with the blind side generally growing faster in length and weight than the eyed side (Sogard, 1991; Fischer and Thompson, 2004; Helling *et al.,* 2005; Mille *et al.,* 2015).

In contrast, in bilaterally symmetrical organisms, i.e. most vertebrates including roundfishes, symmetry is expected to be the rule and to be maintained by homeostasis processes (Palmer, 2009). Deviations from bilateral symmetry in roundfish otolith shape have been reported as potentially resulting from FA and/or DA (Lemberget and Mccormick, 2009; Lychakov, 2013). The origin and consequences of otolith FA on fish remain largely unknown and debated (Díaz-Gil *et al.,* 2015), although it has been documented in several fish species and is regularly associated with stress and/or environmental heterogeneity and thus thought as an indicator of developmental instability (Downhower *et al.,* 1990; Lemberget and Mccormick, 2009; Green *et al.,* 2017). Lemberget and McCormick (2009) supported that otolith FA could be considered as a sensitive indicator of fish health that directly affects the fish performance because otoliths are essential to balance and hearing. More studies need to be carried out to improve the understanding of otolith FA, including its sources and effects.

Regarding DA, which is a consistent bias towards one side, even less is known regarding its potential origin in roundfishes. Although it has been observed in some previous studies, it was only considered as a nuisance in otolith shape analysis and not considered further. Specifically, there was no study trying to identify potential geographical or phylogenetic patterns in otolith DA in roundfishes. This study shows that DA can be observed for one roundfish species in some geographical areas, whereas it is not in others. In addition, the direction of DA can change according to the geographical area where it is detected. Although it is difficult to say whether these results could be generalized to other roundfish species, they suggest that variability in otolith DA in bogue at least could be related to population geographical structuration and thus could be a phenotypically plastic response to environmental drivers, such as temperature, current patterns and food availability, and/or result from genetic differentiation between geographical locations.

Whether varying DA across geographical location results from adaptive or passive phenotypic plasticity and/or adaptive or neutral genetic differentiation is then an open question. Otolith shape asymmetry, be it FA or DA, could generate some dysfunction of the vestibular sensing (Hilbig *et al.,* 2011). Notably, otolith asymmetry affects the acoustic functionality (sensitivity, temporal processing, and sound localization) (Lychakov and Rebane, 2005; Lychakov *et al.,* 2008) and is related to kinetotic swimming of fish (aberrant movement pattern or static space sickness) (Anken *et al.,* 1998; Beier *et al.,* 2002; Hilbig *et al.,* 2003, 2011). In contrast, no obvious advantage of otolith asymmetry has been put forward in the literature, which suggests that, be it of plastic or genetic origin, otolith DA in roundfishes could be non-adaptive.

Stock structure of bogue in the Mediterranean Sea and the Atlantic Ocean

The stock structure revealed by shape analysis of the right otoliths was similar to that obtained when using otoliths from both sides. Three different stocks were identified: North-Western Mediterranean Sea (from the Gulf of Lions to the Tyrrhenian Sea), Central-Eastern Atlantic Ocean and South-Western Mediterranean Sea (from the Canary Islands to the Gulf of Tunis), and Eastern Mediterranean Sea (from the Ionian Sea to the Aegean Sea). This stock structure is similar to that observed for other species in the same areas such as sardine or cephalopods (see Jemaa *et al.,* 2015; Keller *et al.,* 2017). Ider *et al.* (2017) analysing only the data from the Algerian coasts, identified only one stock for this area just as this study conducted at much larger geographic scale, which indicates consistency of otolith shape-based stock discrimination across multiple geographic scales. Factors structuring bogue stocks at the level of the Mediterranean region seem to be linked to environmental features, notably physical oceanographic characteristics of the studied area. The Mediterranean Sea presents a complex circulation pattern. In the South-Western Mediterranean Sea, the environmental conditions are directly influenced by oceanographic processes (Catalan *et al.,* 2013) with the entrance of the Atlantic current being the main forcing agent modulating hydrological processes (García-Lafuente *et al.,* 1998). This exchange of water masses creates the

Almeria-Oran front, with Atlantic water entering the Mediterranean Sea at the surface (up to 150–200 m), and generates a strong current that feeds the Algerian current. This circulation pattern could explain the presence of one stock unit from the Canary Islands to the Algerian coast and its isolation from one stock unit in the North-Western Mediterranean Sea, the latter being also under the influence of the Northern current. The Sicily Channel is a known physical barrier between the western and the eastern basins of the Mediterranean Sea because of its relatively low depth and its peculiar circulation pattern. Regarding the latter, it is under the mixed influence of the Atlantic Ocean current in the western part and, conversely, of the Levantine Intermediate Water (LIW) current, which moves water masses from east to west, in the eastern part (Skliris, 2014). This would explain the separation of the eastern Mediterranean stock from the two more western ones. On top of the hydrological regime, variations in environmental conditions are also likely to play a major role in the observed differences in otolith shape within the studied geographic areas. Water temperature is a key factor influencing primary production in the Mediterranean Sea and these two factors combined are important drivers of fish growth. The average annual sea surface temperature (SST from 2013 to 2016, sampling period, Supplementary Figure S3) exhibited a clear gradient between the northwestern and the southeastern parts of the Mediterranean Sea with higher values along the Levantine coast (Shaltout and Omstedt, 2014). Conversely, primary production (measured as average annual chlorophyll-a concentration) decreased along a gradient from the North-Western Mediterranean Sea characterized by oligotrophic waters to the southeastern Mediterranean Sea identified as ultraoligotrophic waters (Supplementary Figure S4; Stambler, 2014). As for the circulation pattern, the Sicily Channel stands out as a transition zone in terms of environmental conditions. It is characterized by intermediate temperatures (Supplementary Figure S2) and a mix of high primary production along the Tunisian coasts, and more specifically in the Gulf of Gabes, and low primary production in the rest of the Channel (Supplementary Figure S3), which generates some variations of the food web in the area (Rumolo *et al.,* 2017). The higher rate of misclassification of fish sampled in Tunisia is likely to result from the transitional nature of the Sicily Channel in terms of circulation and environmental conditions.

These results highlight the importance of taking into account potential otolith DA when using otolith shape analysis for fish stock identification. Our analyses suggest that there are three bogue stocks in the study area that are geographically coherent and make sense relative to the circulation pattern and environmental conditions in the Mediterranean Sea when using right otoliths or otoliths of both sides together, whereas no population structuration is found when using left otoliths. These results about bogue population structure would need to be confirmed by further studies including genetic analyses of specimens included in the otolith shape analysis and/or otolith microchemistry.

Supplementary data

Supplementary material is available at the *ICESJMS* online version of the manuscript.

Acknowledgements

References

Anken, R., Kappel, T., and Rahmann, H. 1998. Morphometry of fish inner ear otoliths after development at 3 g hypergravity. Acta Oto-Laryngologica, 118: 534–539.

Bao, B., Ke, Z., Xing, J., Peatman, E., Liu, Z., Xie, C., Xu, B. , et al. 2011. Proliferating cells in suborbital tissue drive eye migration in flatfish. Developmental Biology, 351: 200–207.

Begg, G. A., and , and Brown, R. W. 2000. Stock identification of haddock *Melanogrammus aeglefinus* on Georges Bank based on otolith shape analysis. Transactions of the American Fisheries Society, 129: 935–945.

Beier, M., Anken, R., and , and Rahmann, H. 2002. Susceptibility to abnormal (kinetotic) swimming in fish correlates with inner ear carbonic anhydrase-reactivity. Neuroscience Letter, 335: 17–20.

Benzinou, A., Carbini, S., Nasreddine, K., Elleboode, R., and , and Mahé, K. 2013. Discriminating stocks of striped red mullet (*Mullus surmuletus*) in the Northwest European seas using three automatic shape classification methods. Fisheries Research, 143: 153–160.

Bird, J. L., Eppler, D. T., and Checkley, D. M. 1986. Comparisons of herring otoliths using Fourier series shape analysis. Canadian Journal of Fisheries and Aquatic Sciences, 43: 1228–1234.

Bivand, R. S., Pebesma, E., and Gomez-Rubio, V. 2013. Applied Spatial Data Analysis with R, 2nd edn. Springer, New York. 405 pp.

Borcard, D., Gillet, F., and Legendre, P. 2011. Numerical Ecology with R. Springer, New York, Dordrecht, London, Heidelberg. 306 pp.

Bolles, K. L., and Begg, G. A. 2000. Distinction between silver hake (Merluccius bilineariz) stocks in U.S. waters of the northwest Atlantic using whole otolith morphometric. Fishery Bulletin, 98: 451–462.

Bostanci, D., Yilmaz, M., Yedier, S., Kurucu, G., Kontas, S., Darçin, M., and Polat, N. 2016. Sagittal otolith morphology of sharpsnout seabream *Diplodus puntazzo* (Walbaum, 1792) in the Aegean Sea. International Journal of Morphology, 34: 484–488.

Boudinar, A. S., Chaoui, L., Mahé, K., Cachera, M., and Kara, M. H. 2015. Habitat discrimination of big-scale sand smelt *Atherina boyeri* Risso, 1810 (Atheriniformes: Atherinidae) in eastern Algeria using somatic morphology and otolith shape. Italian Journal of Zoology, 82: 446–453.

Burke, N., Brophy, D., and King, P. A. 2008. Otolith shape analysis: its application for discriminating between stocks of Irish Sea and Celtic Sea herring (*Clupea harengus*) in the Irish Sea. ICES Journal of Marine Science, 65: 1670–1675.

Cadrin, S. X., and Friedland, K. D. 1999. The utility of image processing techniques for morphometric analysis and stock identification. Fisheries Research, 43: 129–139.

Cadrin, S. X., Kerr, L. A., and Mariani, S. 2014. Stock Identification Methods: Applications in Fishery Science, 2nd edn. Elsevier Academic Press, Amsterdam. 566 pp.

Campana, S. E., and Neilson, J. D. 1985. Microstructure of fish otoliths. Canadian Journal of Fisheries and Aquatic Sciences, 42: 1014–1032.

Campana, S. E., and Casselman, J. M. 1993. Stock discrimination using otolith shape analysis. Canadian Journal of Fisheries and Aquatic Sciences, 50: 1062–1083.

Campana, S. E. 1999. Chemistry and composition of fish otoliths: pathways, mechanisms and applications. Marine Ecology Progress Series, 188: 263–297.

Capoccioni, F., Costa, C., Aguzzi, J., Menesatti, P., Lombarte, A., and Ciccotti, E. 2011. Ontogenetic and environmental effects on otolith shape variability in three Mediterranean European eel (*Anguilla anguilla*, L.) populations. Journal of Experimental Marine Biology and Ecology, 397: 1–7.

Cardinale, M., Doerin-Arjes, P., Kastowsky, M., and Mosegaard, H. 2004. Effects of sex, stock, and environment on the shape of

known-age Atlantic cod (*Gadus morhua*) otoliths. Canadian Journal of Fisheries and Aquatic Sciences, 61: 158–167.

Casselman, J. M. 1987. Determination of age and growth. *In* The Biology of Fish Growth, pp. 209–242. Ed. by A. H. Weatherley and , and H. S. Gill. Academic Press, New York. 443 pp.

Castonguay, M., Simard, P., and Gagnon, P. 1991. Usefulness of Fourier analysis of otolith shape for Atlantic mackerel (*Scomber scombrus*) stock discrimination. Canadian Journal of Fisheries and Aquatic Sciences, 48: 296–302.

Catalan, I. A., Macias, D., Sole, J., Ospina-Alvarez, A., and Ruiz, J. 2013. Stay off the motorway: resolving the pre-recruitment life history dynamics of the European anchovy in the SW Mediterranean through a spatially-explicit individual-based model (SEIBM). Progress in Oceanography, 111: 140–153.

de Pontual, H., and Prouzet, P. 1987. Atlantic salmon (*Salmo salar* L.) stock discrimination by scale shape analysis. Aquaculture and Fisheries Management, 18: 227–289.

de Pontual, H., and Prouzet, P. 1988. Numerical analysis of scale morphology to discriminate between Atlantic salmon stocks. Aquatic Living Resources, 1: 17–27.

Díaz-Gil, C., Palmer, M., Catalán, I. A., Alós, J., Fuiman, L. A., García, E., del Mar Gil, M. , *et al.* 2015. Otolith fluctuating asymmetry: a misconception of its biological relevance? ICES Journal of Marine Science, 72: 2079–2089.

Dimarchopoulou, D., Stergiou, K. I., and Tsikliras, A. C. 2017. Gap analysis on the biology of Mediterranean marine fishes. PLoS One, 12: e0175949.

Downhower, J. F., Blumer, L. S., Lejeune, P., Gaudin, P., Marconato, A., and Bisazza, A. 1990. Otolith asymmetry in *Cottus bairdi* and *Cottus gobio*. Polskie Archiwum Hydrobiologii, 37: 209–220.

Duarte-Neto, P., Lessa, R., Stosic, B., and Morize, E. 2008. The use of sagittal otoliths in discriminating stocks of common dolphinfish (*Coryphaena hippurus*) off northeastern Brazil using multishape descriptors. ICES Journal of Marine Science, 65: 1144–1152.

FAO. 2016. The State of Mediterranean and Black Sea Fisheries (2016) (SoMFi (2016)). Food and Agriculture Organization of the United Nations, Rome. 152 pp.

Fischer, A. J., and Thompson, B. A. 2004. The age and growth of southern flounder, *Paralichthys lethostigma*, from Louisiana estuarine and offshorewaters. Bulletin of Marine Science, 75: 63–77.

Fox, J. 2003. Effect displays in R for generalised linear models. Journal of Statistical Software, 8: 1–18.

Fox, J., and Weisberg, S. 2011. An {R} Companion to Applied Regression, 2nd edn. SAGE, Thousand Oaks, CA. 472 pp.

Gagliano, M., and McCormick, M. I. 2004. Feeding history influences otolith shape in tropical fish. Marine Ecology Progress Series, 278: 291–296.

Garcia, A., Mattiucci, S., Damiano, S., Santos, M. N., and Nascetti, G. 2011. Metazoan parasites of swordfish, *Xiphias gladius* (Pisces: Xiphiidae) from the Atlantic Ocean: implications for host stock identification. ICES Journal of Marine Science, 68: 175–182.

García-Lafuente, J., Vargas, J. M., Cano, N., Sarhan, T., Plaza, F., and Vargas, M. 1998. Observaciones de corriente en la estación 'N' en el Estrecho de Gibraltar desde Octubre de (1995) a Mayo de (1996). Informes Técnicos. Instituto Español de Oceanografía, 169: 1–46.

Govind, C. K., and Pearce, J. 1986. Differential reflex activity determines claw and closer muscle asymmetry in developing lobsters. Science, 233: 354–356.

Green, A. A., Mosaliganti, K. R., Swinburne, I. A., Obholzer, N. D., and Megason, S. G. 2017. Recovery of shape and size in a developing organ pair. Developmental Dynamics, 246: 451–465.

Helling, K., Scherer, H., Hausmann, S., and Clarke, A. H. 2005. Otolith mass asymmetries in the utricle and saccule of flatfish. Journal of Vestibular Research, 15: 59–64.

Hilbig, R., Anken, R., and Rahmann, H. 2003. On the origin of susceptibility to kinetotic swimming behaviour in fish: A parabolic aircraft flight study. Journal of Vestibular Research, 12: 185–189.

Hilbig, R., Knie, M., Shcherbakov, D., and Anken, R. H. 2011. Analysis of behaviour and habituation of fish exposed to diminished gravity in correlation to inner ear stone formation—a sounding rocket experiment (TEXUS 45). In Proceedings of the 20th ESA Symposium on European Rocket and Balloon Programmes and Related Research, 22–26 May (2011), Hyere, France.

Hüssy, K. 2008. Otolith shape in juvenile cod (*Gadus morhua*): ontogenetic and environmental effects. Journal of Experimental Marine Biology and Ecology, 364: 35–41.

Hutchings, J. A. 2005. Life history consequences of overexploitation to population recovery in Northwest Atlantic cod (*Gadus morhua*). Canadian Journal of Fisheries and Aquatic Sciences, 62: 824–832.

ICES. 2016. Report of the Stock Identification Methods Working Group (SIMWG). ICES CM (2016)/SSGEPI: 16. 47 pp.

Ider, D., Ramdane, Z., Mahé, K., Duffour, J. L., Bacha, M., and Amara, R. 2017. Use of otolith shape analysis to discriminate stocks of *Boops boops* (L.) from the Algerian coast (southwestern part of the Mediterranean Sea). African Journal of Marine Science, 39: 251–258.

Jemaa, S., Bacha, M., Khalaf, G., Dessailly, D., Rabhi, K., and Amara, R. 2015. What can otolith shape analysis tell us about population structure of the European sardine, *Sardina pilchardus*, from Atlantic and Mediterranean waters? Journal of Sea Research, 96: 11–17.

Keller, S., Quetglas, A., Puerta, P., Bitetto, I., Casciaro, L., Cuccu, D., Esteban, A. , *et al.* 2017. Environmentally driven synchronies of Mediterranean cephalopod populations. Progress in Oceanography, 152: 1–14.

Klecka, W. R. 1980. Discriminant Analysis. Sage Publications, Beverly Hills, CA.

Kuhl, F., and Giardina, C. 1982. Elliptic Fourier features of a closed contour. Computer Graphics and Image Processing, 18: 236–258.

Legendre, P., and Legendre, L. F. J. 1998. Numerical Ecology. 2nd edn. Elsevier Science, Amsterdam, Netherlands. 853 pp.

Lemberget, T., and Mccormick, M. I. 2009. Replenishment success linked to fluctuating asymmetry in larval fish. Oecologia, 159: 83–93.

Lestrel, P. E. 2008. Fourier Descriptors and Their Applications in Biology. Cambridge University Press, Cambridge. 460 pp.

Lombarte, A., and Lleonart, J. 1993. Otolith size changes related with body growth, habitat depth and temperature. Environmental Biology of Fishes, 37: 297–306.

Lychakov, D. V., and Rebane, Y. T. 2005. Fish otolith mass asymmetry: morphometry and influence on acoustic functionality. Hearing Research, 201: 55–69.

Lychakov, D. V., Rebane, Y. T., Lombarte, A., Demestre, M., and Fuiman, L. A. 2008. Saccular otolith mass asymmetry in adult flatfishes. Journal of Fish Biology, 72: 2579–2594.

Lychakov, D. 2013. Behavioral lateralization and otolith asymmetry. Journal of Evolutionary Biochemistry and Physiology, 49: 441–456.

Mahé, K., Evano, H., Mille, T., Muths, D., and Bourjea, J. 2016. Otolith shape as a valuable tool to evaluate the stock structure of swordfish *Xiphias gladius* in the Indian Ocean. African Journal of Marine Science, 38: 457–464.

Mapp, J., Fisher, M., Bagnall, A., Lines, J., Warne, S., and Phillips, J. S. 2013. *Clupea harengus*: intraspecies distinction using curvature scale space and shapelets-classification of North-Sea and Thames herring using boundary contour of sagittal otoliths. Proc. 2nd International Conference on Pattern Recognition Applications and Methods (ICPRAM (2013)).

Mapp, J., Hunter, E., Van Der Kooij, J., Songer, S., and Fisher, M. 2017. Otolith shape and size: the importance of age when determining indices for fish-stock separation. Fisheries Research, 190: 43–52.

Massou, A. M., Le Bail, P. Y., Panfili, J., Laë, R., Baroiller, J. F., Mikolasek, O., Fontenelle, G. , et al. 2004. Effects of confinement stress of variable duration on the growth and microincrement deposition in the otoliths of *Oreochromis niloticus* (Cichlidae). Journal of Fish Biology, 65: 1253–1269.

Mérigot, B., Letourneur, Y., and Lecomte-Finiger, R. 2007. Characterization of local populations of the common sole *Solea solea* (Pisces, Soleidae) in the NW Mediterranean through otolith morphometrics and shape analysis. Marine Biology, 151: 997–1008.

Mille, T., Mahé, K., Villanueva, C. M., De Pontual, H., and Ernande, B. 2015. Sagittal otolith morphogenesis asymmetry in marine fishes. Journal of Fish Biology, 87: 646–663.

Mille, T., Mahé, K., Cachera, M., Villanueva, C. M., De Pontual, H., and Ernande, B. 2016. Diet is correlated with otolith shape in marine fish. Marine Ecology Progress Series, 555: 167–184.

Monteiro, L. R., Di Beneditto, A. P. M., Guillermo, L. H., and Rivera, L. A. 2005. Allometric changes and shape differentiation of sagitta otoliths in sciaenid fishes. Fishery Research, 74: 288–299.

Oksanen, J., Blanchet, F. G., Kindt, R., Legendre, P., Minchin, P. R., O'Hara, R. B., Simpson, G. L. , et al. 2013. Vegan: Community Ecology Package. R package version 2.0–10. 292 pp.

Palmer, A. R., and Strobeck, C. 1986. Fluctuating asymmetry: measurement, analysis, patterns. Annual Review of Ecology and Systematics, 17: 391–421.

Palmer, A. R., and Strobeck, C. 1992. Fluctuating asymmetry as a measure of developmental stability implications of non-normal distributions and power of statistical tests. Acta Zoologica Fennica, 191: 57–72.

Palmer, A. R. 2009. Animal asymmetry. Current Biology, 19: 473–477.

Parisi-Baradad, V., Lombarte, A., Garcia-Ladona, E., Cabestany, J., Piera, J., and Chic, O. 2005. Otolith shape contour analysis using affine transformation invariant wavelet transforms and curvature scale space representation. Marine Freshwater Research, 56: 795–804.

Pawson, M. G., and Jennings, S. 1996. A critique of methods for stock identification in marine capture fisheries. Fisheries Research, 25: 3–4.

Petursdottir, G., Begg, G. A., and Marteinsdottir, G. 2006. Discrimination between Icelandic cod (*Gadus morhua* L.) populations from adjacent spawning areas based on otolith growth and shape. Fisheries Research, 80: 182–189.

Pinheiro, J., Bates, D., DebRoy, S., and Sarkar, D. 2016. nlme: Linear and Nonlinear Mixed Effects Models. R Package Version, 3.1–128.

Pita, A., Casey, J., Hawkins, S. J., Villarreal, M. R., Gutiérrez, M.-J., Cabral, H., Carocci, F., et al. 2016. Conceptual and practical advances in fish stock delineation. Fisheries Research, 173: 185–193.

Ponton, D. 2006. Is geometric morphometrics efficient for comparing otolith shape of different fish species? Journal of Morphology, 267: 750–757.

Ramirez-Perez, J. S., Quinonez-V, C., Garcia-Rod, F. J., Felix-Urag, R., and Melo-Barre, F. N. 2010. Using the shape of sagitta otoliths in the discrimination of phenotypic stocks in *Scomberomorus sierra* (Jordan and Starks, 1895). Canadian Journal of Fisheries and Aquatic Sciences, 5: 82–93.

R Development Core Team, 2016. R: A Language and Environment for Statistical Computing. R Foundation for Statistical Computing,. Vienna, Austria.

Rebaya, M., Ben Faleh, A. R., Allaya, H., Khedher, M., Trojette, M., Marsaoui, B., Fatnassi, M., et al. 2017. Otolith shape discrimination of *Liza ramada* (Actinopterygii: Mugiliformes: Mugilidae) from marine and estuarine populations in Tunisia. Acta Ichthyologica et Piscatoria, 47: 13–21.

Reiss, H., Hoarau, G., Dickey-Collas, M., and Wolff, W. 2009. Genetic population structure of marine fish: mismatch between biological and fisheries management units. Fish and Fisheries, 10: 361–395.

Rencher, A. C., and Christensen, W. F. 2012. Methods of Multivariate Analysis, 3rd edn. Wiley, New York. 800 pp.

Rohlf, F. J., and Archie, J. W. 1984. A comparison of Fourier methods for the description of wing shape in mosquitoes (Diptera: Culicidae). Systematic Biology, 33: 302–317.

Rumolo, P., Basilone, G., Fanelli, E., Barra, M., Calabrò, M., Genovese, S., Gherardi, S. , et al. 2017. Linking spatial distribution and feeding behavior of Atlantic horse mackerel (*Trachurus trachurus*) in the Strait of Sicily (Central Mediterranean Sea). Journal of Sea Research, 121: 47–58.

Sadighzadeh, Z., Valinassab, T., Vosugi, G., Motallebi, A. A., Fatemi, M. R., Lombarte, A., and Tuset, V. M. 2014. Use of otolith shape for stock identification of John's snapper, *Lutjanus johnii* (Pisces: Lutjanidae), from the Persian Gulf and the Oman Sea. Fisheries Research, 155: 59–63.

Shaltout, M., and Omstedt, A. 2014. Recent sea surface temperature trends and future scenarios for the Mediterranean Sea. Oceanologia, 56: 411–443.

Silva, A., Skagen, D. W., Uriarte, A., Massé, J., Santos, M. B., Marques, V., Carrera, P. , et al. 2009. Geographic variability of sardine dynamics in the Iberian Biscay region. ICES Journal of Marine Science, 66: 495–508.

Simoneau, M., Casselman, J. M., and Fortin, R. 2000. Determining the effect of negative allometry (length/height relationship) on variation in otolith shape in lake trout (*Salvelinus namaycush*), using Fourier-series analysis. Canadian Journal of Zoology, 78: 1597–1603.

Skliris, N. 2014. Past, present and future patterns of the thermohaline circulation and characteristic water masses of the Mediterranean sea. *In* The Mediterranean Sea—Its History and Present Challenges, pp. 29–48. Ed. by S. Goffredo and , and Z. Dubinky. Springer, Dordrecht, Heidelberg, New York, London. 678 pp.

Smith, M. K. 1992. Regional differences in otolith morphology of the deep slope red snappers *Etelis carbunculus*. Canadian Journal of Fisheries and Aquatic Sciences, 49: 795–804.

Sogard, S. M. 1991. Interpretation of otolith microstructure in juvenile winter flounder (*Pseudopleuronectes americanus*): ontogenetic development, daily increment validation, and somatic growth relationships. Canadian Journal of Fisheries and Aquatic Sciences, 48: 1862–1871.

Stambler, N. 2014. The Mediterranean Sea—primary productivity. *In* The Mediterranean Sea—Its History and Present Challenges, pp. 113–121. Ed. by S. Goffredo and , and Z. Dubinky. Springer, Dordrecht, Heidelberg, New York, London. 678 pp.

Stephenson, R. L., Rodman, K., Aldous, D. G., and Lane, D. E. 1999. An in-season approach to management under uncertainty: the case of the SW Nova Scotia herring fishery. ICES Journal of Marine Science, 56: 1005–1013.

Swan, S., Geffen, A., Moralesnin, B., Gordon, J., Shimmield, T., Sawyer, T., and Massuti, E. 2006. Otolith chemistry: an aid to stock separation of *Helicolenus dactylopterus* (Bluemouth) and *Merluccius merluccius* (European hake) in the Northeast Atlantic and Mediterranean. ICES Journal of Marine Science, 63: 504–513.

Todorov, V., and Filzmoser, P. 2009. An object-oriented framework for robust multivariate analysis. Journal of Statistical Software, 32: 1–47.

Torres, G. J., Lombarte, A., and Morales-Nin, B. 2000. Sagittal otolith size and shape variability to identify geographical intra-specific differences in three species of genus *Merluccius*.

Journal of the Marine Biological Association of the UK, 80: 333–342.

Trojette, M., Ben Faleh, A., Fatnassi, M., Marsaoui, B., Mahouachi, N. H., Chalh, A., Quignard, J.-P. , et al. 2015. Stock discrimination of two insular populations of *Diplodus annularis* (Actinop-terygii: Perciformes: Sparidae) along the coast of Tunisia by analysis of otolith shape. Acta Ichthyologica et Piscatoria, 45: 363–372.

Tuset, V. M., Lozano, I. J., Gonzalez, J. A., Pertusa, J. F., and García-Dıaz, M. M. 2003. Shape indices to identify regional differences in otolith morphology of comber, *Serranus cabrilla* (L., 1758). Journal of Applied Ichthyology, 19: 88–93.

Venables, W. N., and Ripley, B. D. 2002. Modern Applied Statistics with S, 4th edn. Springer, New York. 446 pp.

Vergara-Solana, F. J., García-Rodríguez, F. J., and De La Cruz-Agüero, J. 2013. Comparing body and otolith shape for stock discrimination of Pacific sardine, *Sardinops sagax* Jenyns, 1842. Journal of Applied Ichthyology, 29: 1241–1246.

Vignon, M., and Morat, F. 2010. Environmental and genetic determinant of otolith shape revealed by a non-indigenous tropical fish. Marine Ecology Progress Series, 411: 231–241.

Vignon, M. 2018. Short-term stress for long-lasting otolith morphology—brief embryological stress disturbance can reorient otolith ontogenetic trajectory. Canadian Journal of Fisheries and Aquatic Sciences, 75: 1713–1722.

Wang, Y. J., Ye, Z. J., Liu, Q., and Cao, L. 2011. Stock discrimination of spotted tail goby (*Synechogobius ommaturus*) in the Yellow Sea by analysis of otolith shape. Oceanologia et Limnologia Sinica, 29: 192–198.

Whitehead, P. J. P., Bauchot, M. L., Hureau, J. C., Nielsen, J., and Tortonese, E. 1984. Fishes of the North-Eastern Atlantic and the Mediterranean. UNESCO, Paris. 510 pp.

Wickham, H. 2016. ggplot2: Elegant Graphics for Data Analysis. Springer-Verlag, New York. 182 pp.

Wooster, W. S. 1992. King crab dethroned. *In* Climate, Variability, Climate Change and Fisheries, pp. 14–30. Ed. by M. H. Glantz. Cambridge University Press, New York. 458 pp.

Zhang, C., Ye, Z., Li, Z., Wan, R., Ren, Y., and Dou, S. 2016. Population structure of Japanese Spanish mackerel *Scomberomorus niphonius* in the Bohai Sea, the Yellow Sea and the East China Sea: evidence from random forests based on otolith features. Fisheries Science, 82: 251–256.

Handling editor: Francis Juanes